applied sciences

MDPI

Article

Online Learning-Based Adaptive Device-Free Localization in Time-Varying Indoor Environment

Jianqiang Xue [1], Xingcan Chen [1], Qingyun Chi [2,*] and Wendong Xiao [1,3,4,*]

[1] School of Automation and Electrical Engineering, University of Science and Technology Beijing, Beijing 100083, China; b20170301@xs.ustb.edu.cn (J.X.); d202210337@xs.ustb.edu.cn (X.C.)
[2] School of Information Science and Engineering, Zaozhuang University, Zaozhuang 277160, China
[3] Beijing Engineering Research Center of Industrial Spectrum Imaging, Beijing 100083, China
[4] Shunde Innovation School, University of Science and Technology Beijing, Shunde 528399, China
* Correspondence: 100951@uzz.edu.cn (Q.C.); wdxiao@ustb.edu.cn (W.X.)

Abstract: With the widespread use of WiFi devices and the availability of channel state information (CSI), CSI-based device-free localization (DFL) has attracted lots of attention. Fingerprint-based localization methods are the primary solutions for DFL, but they are faced with the fingerprint similarity problem due to the complex environment and low bandwidth of the commercial WiFi. Meanwhile, fingerprints may change unpredictably due to multipath WiFi signal propagation in time-varying environments. To tackle these problems, this paper proposes an adaptive online learning DFL method, which adaptively updates the localization model to ensure long-term accuracy and adaptability. Specifically, the CSI signals of the target located at different reference points are first collected and transformed to discriminable fingerprints using the weights of Multilayer Online Sequence Extreme Learning Machine (ML-OSELM). After that, an online learning DFL model is built to adapt to the changes of the environment. Experimental results in a time-varying indoor environment validate the adaptability of the proposed method against environmental changes and show that our method can achieve 10% improvement over other methods.

Keywords: device-free localization (DFL); channel state information (CSI); fingerprint similarity problem; environmental changes; Multilayer Online Sequence Extreme Learning Machine (ML-OSELM)

Citation: Xue, J.; Chen, X.; Chi, Q.; Xiao, W. Online Learning-Based Adaptive Device-Free Localization in Time-Varying Indoor Environment. *Appl. Sci.* **2024**, *14*, 643. https://doi.org/10.3390/app14020643

Academic Editors: Juan-Carlos Cano and Alessandro Lo Schiavo

Received: 13 September 2023
Revised: 17 December 2023
Accepted: 4 January 2024
Published: 12 January 2024

1. Introduction

With the rapid development of society and the rapid iteration of electronic devices, people's demand for quality of life is becoming higher, and numerous kinds of new services and demands have emerged. Location-Based Service (LBS) technology is an important support for these services, and the number of production and life activities based on LBS has increased rapidly [1]. How to accurately obtain the location of the target over a long term is the fundamental task of LBS-based services.

Global Positioning System (GPS) signals are the main method of localization in daily life nowadays, but GPS signals are easily affected by buildings and cannot play well in the indoor environment [2]. With the development of society, there are more large buildings, and the area of the indoor environment is further expanded. More and more researchers gradually turned the focus of research to the indoor localization technology. Infrared technology, Wireless Local Area Networks (WLAN) technology, camera technology, Bluetooth technology, ultra-wideband (UWB) technology, and ZigBee technology all shine in indoor localization [3]. Specifically, Bluetooth and infrared-based technologies only have a small coverage area. Camera-based technology needs good lighting conditions and will cause discomfort for the target. UWB and ZigBee-based technologies require complex deployment due to the requirement to consider issues such as placement spacing, height, and the orientation of multiple devices during localization, limiting their practical application scenarios. Technology based on specialized equipment can achieve high-precision localization,

but it is expensive [4]. The first problem in the implementation of the indoor localization technology is the deployment of wireless devices. Among the above wireless technologies, WiFi-based technology has a wide range of commercial applications and requires only a small number of devices. For example, Linksys [5] sells mesh WiFi devices and provides a service called "Linksys Aware", which enables WiFi devices to monitor movement around the house and informs users when meaningful motion is detected, but it cannot provide the location of the target. Therefore, WiFi-based indoor localization technology has become a promising alternative technology for indoor localization [6].

WiFi-based indoor localization methods are divided into active indoor localization and passive indoor localization [7]. The active indoor localization methods require that the target is equipped with devices that can receive wireless signals and locate the target by identifying the location of the equipment [8]. Passive localization is also known as device-free localization (DFL), where the target does not need to wear any device and has a wide range of applications. Passive indoor localization is necessary in situations where signals are poor or cell phones are restricted, such as mines, but the location of the target may be still needed in these situations. WiFi-based DFL uses Received Signal Strength (RSS) or Channel State Information (CSI) as a localization indicator. RSS has the characteristics of simple collection and easy calculation, but the collected data itself have significant instability due to the multipath effect, NLOS effect, complex environment and different hardware designs [9]. RSS is not particularly sensitive to the perception of subtle movements, which may lead to the same localization results when the target moves in a small area [10]. Compared with RSS, CSI also suffers from problems such as multipath effects and an NLOS effect, but it includes the amplitude and phase information of multiple subcarriers, which can portray the channel characteristics better than RSS, effectively improving the resolution of multipath signals and further improving the accuracy of the indoor localization [11].

WiFi-based DFL includes two kinds of methods: fingerprint-based and model-based methods [12]. The model-based methods are based on physical laws combined with the actual situation to establish a physical model to estimate the location. This method has high localization accuracy, but it is difficult to adapt to complex environments. The fingerprint-based methods build a fingerprint database from different reference locations and then use machine learning or deep learning to establish a relationship from signal to location. This kind of method has high localization performance under the assumption that fingerprints corresponding to different locations are distinguishable. Therefore, many existing works focus on designing fingerprints. For example, Ding et al. [13] designed a CSI tensor by reconstructing CSI time series through integrating WiFi transmission links, aiming to fully characterize the profiles of the locations of the target. Khalilsarai et al. [14] spliced measured CSI over multiple WiFi bands to construct channel impulse response to achieve high localization accuracy.

However, Wu et al. [15] proves that when WiFi bandwidth is insufficient, signals located at different locations will be ambiguous, causing similarities in fingerprints corresponding to different locations. In our previous work, we analyzed the fingerprint similarity problem using the Fresnel model and proposed a device-free localization method based on deep representation. In this paper, we focus on addressing localization in time-varying environments [16]. We use a pair of transceivers in the home environment to collect information when the target is located at different positions, which are known as reference points. We can locate the target based on the fact that the propagation pattern of the signal will be affected when the target is located at different positions. We use the time-reversal method [15] to quantify the similarity between fingerprints corresponding to different reference points, as shown in Figure 1. The time-reversal method is a signal processing technique, which combines a particular time instance $h(t)$ with its time-reversed and conjugated counterpart $h^*(-t)$ to remove the phase distortion. The time-reversal technique can refocus the energy of signal waves at the intended location, which is known as the spatial focusing effect. The Z-axis depicts the resonance strength between different

reference points, which is the maximal amplitude of the entries of the cross-correlation between two complex signals and 1 is the maximum. From Figure 1, we can find that the fingerprints corresponding to different reference locations have high similarity, where the target's fingerprint cannot be correctly matched with the corresponding location. To address this problem, we propose a DFL model based on deep representation. In the indoor environment, the environment will change due to the influence of the target to the indoor environment, causing changes of propagation paths of WiFi and a degradation of localization accuracy. To address this problem, we propose an OS-ELM-based method to adapt to environmental changes and ensure the adaptability of the model.

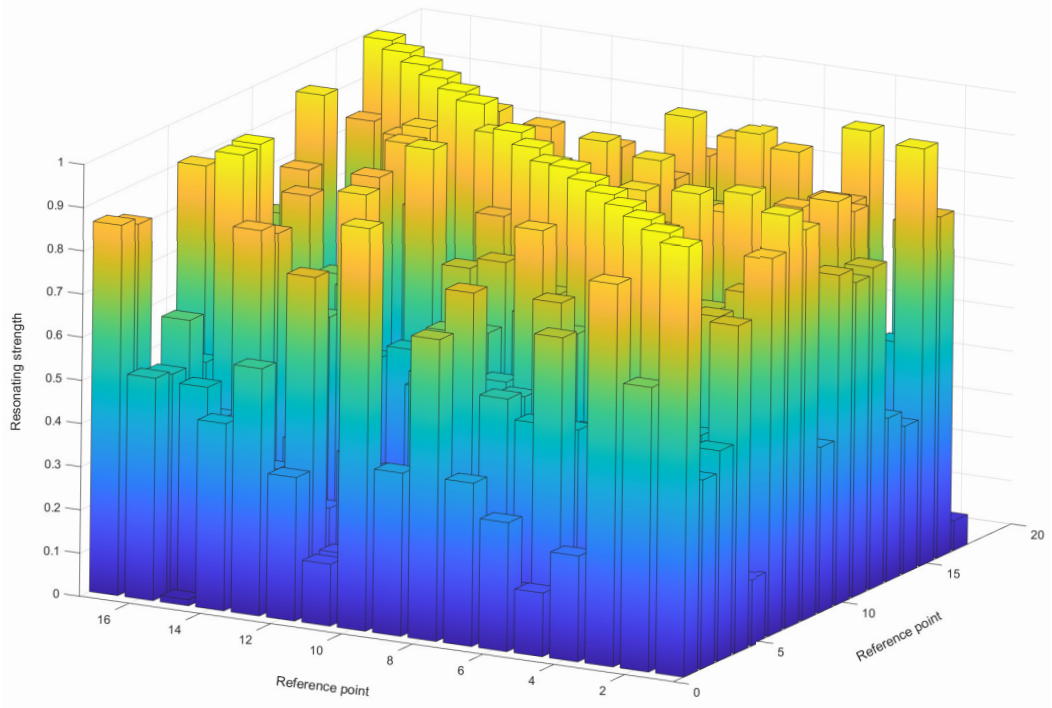

Figure 1. Fingerprint similarity of different reference points. Both the X-axis and Y-axis indicate the serial numbers of reference points, and the Z-axis depicts the similarity of fingerprints between reference points.

In this paper, we make the following main contributions.

- We design a kind of fingerprint based on deep learning weights that can effectively tackle the fingerprint similarity problem.
- We propose an online learning DFL approach that can effectively adapt to time-varying environments.
- We validate our approach using data from real-world environments and demonstrate that our approach outperforms other approaches.

The rest of this paper is organized as follows. Related works are discussed in Section 2. The relevant fundamentals are presented in Section 3. The proposed ML-OSELM-based DFL method is described in Section 4. Performance validation is presented in Section 5. Finally, conclusions and future work are concluded in Section 6.

2. Related Work

WiFi-based DFL is mainly divided into model-based and fingerprint-based methods, and we will introduce DFL methods from these two aspects in the following.

2.1. Model-Based DFL Method

Model-based DFL methods usually use certain physical principles to calculate the relevant physical characteristics of the target, such as speed, angle, distance, etc., from the

original signal, and then they calculate the location of the target from the physical characteristics. This kind of method is a process from original signal to physical characteristics to the location of the target.

Zhang et al. [17] proposed to utilize the freedom provided by the Intelligent Reflecting Surface (IRS), composed of a multitude of controllable reflective elements, to modulate the spatial distribution of WiFi signals. This breaks down the spatial resolution limitation of WiFi signals to achieve accurate localization. Kandel et al. [18] demonstrated, via simulation, that the integration of information from multiple frequency bands (wideband CSI), such as an increase in subcarrier or virtual antenna, significantly enhanced the performance of MUSIC in separating multipath components and improved localization accuracy. Zuo et al. [19] proposed an improved four-dimensional parameter estimation approach based on a two-stage algorithm. They utilized the orthogonal matching pursuit (OMP) for coarse estimation and subsequently employed space-alternating generalized expectation–maximization (SAGE) for parameter refinement, thereby enhancing the accuracy of weak human-induced reflection path parameters. Zhang et al. [20] developed a novel DFT system which refines motion-induced phase shifts from highly noisy CSI measurements to detect the Doppler shift. This system achieved joint Doppler velocity and AOA estimation of the target path within the compressive sensing framework, resulting in high accuracy for target velocity estimation and motion tracking. Model-based methods are capable of explaining the propagation of signals and obtaining accurate localization. However, the model-based methods are not practical in complex environments and difficult to adapt to environmental changes.

2.2. Fingerprint-Based DFL Method

The fingerprint-based DFL methods generally include offline and online phases. In the offline phase, signals from different reference locations are first collected and fingerprints with differentiation are designed to build a fingerprint database. In the online phase, the location of the target is calculated by comparing the difference between the real-time collected values and the fingerprint database. The fingerprint-based methods are used to implement a mapping from signal to location by specific methods.

Ding et al. [21] firstly formulated a shared consistent representation using CSI measurements, employed the singular value decomposition (SVD) method to decompose the consistent representation to obtain distinguishable features, utilized t-distributed stochastic neighbor embedding (t-SNE) to capture hidden structural characteristics, and utilized the AdaBoost model to establish a robust relationship between the input and output for achieving indoor localization. Zhang et al. [22] firstly partitioned the entire environment into multiple subdomains using the K-means clustering method in order to implement large-scale DFL. Subsequently, they proceeded to train a corresponding number of DFL models for each subdomain, utilizing the Fresnel phase difference as the fingerprints. In this way, the large-scale DFL problem can be regarded as conventional DFL problems. In order to fully exploit the potential of the collected data set in DFL, Wu et al. [23] proposed to employ a pixel-level multimodal representation of radio images to fuse both amplitude and phase features. They used a novel Conditional Generative Adversarial Network with Auxiliary Classifier (AC-GAN) model to generate artificial samples for further expanding the collected data set. Additionally, they employed a regression formulation to train the Convolutional Neural Networks (CNNs) for positioning. Shi et al. [24] modeled the CSI change vector as a multivariate Gaussian distribution to analyze a human-induced variance of CSI measurements and used Bayesian filtering techniques to track the trajectory of an individual. Duan et al. [25] proposed data rate (DR) fingerprinting, proposed a time-window mechanism with different fingerprint formulations, designed an access point (AP) switching strategy, and designed a new matching algorithm named dynamic nearest neighbors (DNNs) to achieve DFL.

The above-mentioned works designed fingerprints manually, but it is difficult to address the fingerprint similarity problem by artificial fingerprints. Zeng et al. [26] demonstrate that the ratio-based features can reduce noise and increase the sensing range, so we

transform the raw signal to a ratio-based fingerprint to illustrate the fingerprint similarity problem. In Figure 2, we compare the data of a period of time from one of thirty subcarriers corresponding to different locations. When only a small number of reference points are considered, i.e., three, the raw signals will have a certain degree of similarity, and the ratio-based fingerprints can tackle the fingerprint similarity problem well and distinguish the fingerprints corresponding to different locations, as shown in Figure 2a–c and Figure 2d–f, respectively. The red dots are reference points used for comparison, while the black dots are other reference points. But when there are too many reference points, e.g., six, the raw signals can be quite ambiguous, and the ratio-based features cannot distinguish well between the fingerprints corresponding to the different locations, as shown in Figure 2g–i. In the middle column and right column of Figure 2, the X-axis and Y-axis indicate the real and imaginary parts of the CSI signal, respectively.

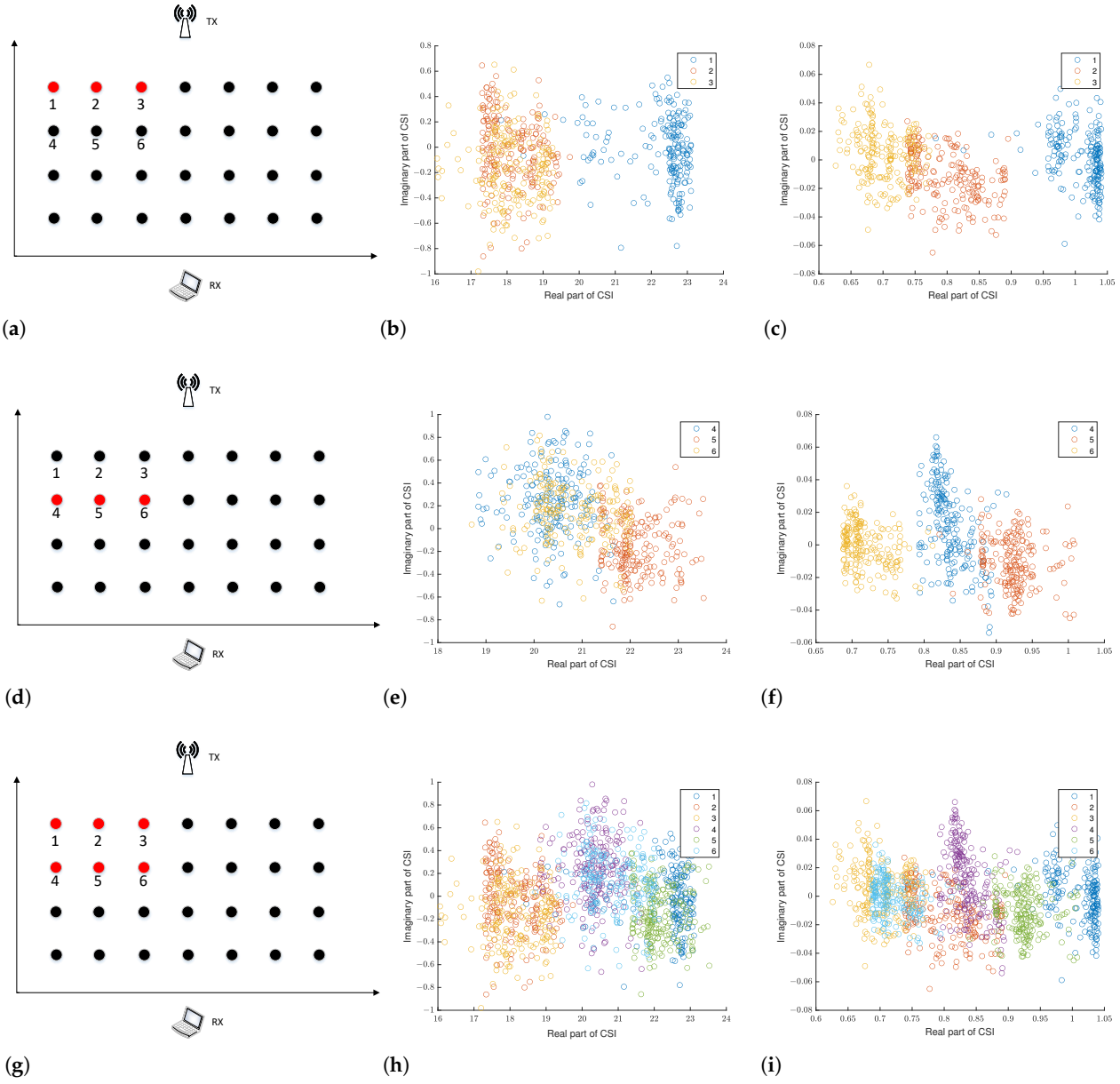

Figure 2. Results of the distinguishability of comparing the raw signal with the ratio-based features. (**a**,**d**,**g**) The schematic diagram of the reference locations; (**b**,**e**,**h**) The original signals distribution of the corresponding reference locations; (**c**,**f**,**i**) the ratio-based features distribution of the corresponding reference locations.

Meanwhile, as the WiFi signals will be impacted by various environmental factors, CSI fingerprints will exhibit significant variations due to environmental changes. Consequently, the accuracy of the DFL model is significantly degraded in the time-varying environment. To address this issue, AdapLoc was proposed, which utilized a one-dimensional Convolutional Neural Network (1D-CNN) and leveraged Domain Adaptation (DA) with Semantic Alignment (SA) to achieve adaptation [27]. However, even when the environment changes due to the movement of furniture or other objects, there is still much room for improving the localization accuracy in the fingerprint-based DFL. Lei et al. [28] proposed a novel DFL algorithm for dynamic environments, featuring an enhanced channel-selection method and adopting the logistic regression classifier to enhance the localization accuracy. The above works can adapt to the changes in the environment but do not address the similarities between fingerprints. In this paper, we construct a discriminable fingerprint with deep learning representation and propose an online learning-based mechanism to design a DFL model against environmental changes in the time-varying environment.

3. Preliminaries

In this section, we introduce CSI and OS-ELM theory to help understand the proposed method.

3.1. CSI Primer

With the use of technologies such as MIMO and OFDM in WiFi networks, it has become possible to obtain CSI in commercial WiFi devices [29]. CSI is a physical quantity that describes the channel properties of the communication link between the transmitter and receiver and describes the fading factor of the signal on each transmission path and characterizes the phase and amplitude information of each subcarrier in the channel [25,30]. The signal transmission model is as follows

$$\mathbf{R} = \mathbf{ZO} + \mathbf{u}, \tag{1}$$

where $\mathbf{R}$ and $\mathbf{O}$ are the received and transmitted signal vectors, respectively, $\mathbf{Z}$ is the channel frequency response matrix and $\mathbf{u}$ is the noise vector. Normally, the channel frequency response needs to be obtained with the help of specialized instruments, but it is now possible to obtain the channel frequency response in the form of channel status information using the CSITool. The channel frequency response can be expressed as

$$\mathbf{Z} = [CSI_1, CSI_2, \ldots CSI_k, \ldots, CSI_M]^T, \tag{2}$$

where M denotes the number of subcarriers in the orthogonal frequency division multiplexing system and CSI_k denotes the frequency response of the kth subcarrier. CSI_k can be expressed as

$$CSI_k = |CSI_k| e^{j\theta_k}, \tag{3}$$

where $|CSI_k|$ is the amplitude information and θ_k is the phase information of the kth subcarrier.

3.2. OS-ELM

OS-ELM was proposed by Liang et al. [31] to learn data individually or in batches, which has a faster learning speed and better generalization performance, and it can learn data online with fixed or varying chunk sizes. OS-ELM is divided into two phases including an initialization phase and online learning phase, whose architecture is shown in Figure 3. In the initialization phase, the input layer to hidden layer weights $\mathbf{w}$ and hidden layer

bias **b** of OS-ELM are first randomly initialized. Given the input **x** and the activation function $g(x)$, the output **H** of the hidden layer can be computed as

$$\begin{aligned}\mathbf{H} &= g(\mathbf{x};\mathbf{w},\mathbf{b}) \\ &= \begin{bmatrix} g(\mathbf{w}_1^{\mathrm{T}}\mathbf{x}_1 + b_1) & \cdots & g(\mathbf{w}_L^{\mathrm{T}}\mathbf{x}_1 + b_L) \\ \vdots & \vdots & \vdots \\ g(\mathbf{w}_1^{\mathrm{T}}\mathbf{x}_N + b_1) & \cdots & g(\mathbf{w}_L^{\mathrm{T}}\mathbf{x}_N + b_L) \end{bmatrix}_{N\times L},\end{aligned} \tag{4}$$

where N is the number of samples; L is the number of the hidden layer nodes and T denotes the transpose of the matrix.

The hidden layer to output layer weights can be expressed as

$$\beta^{(0)} = \mathbf{P}_0 {\mathbf{H}_0}^T \mathbf{Y}_0, \tag{5}$$

where $\mathbf{Y}_0$ is the label corresponding to the training data, $\mathbf{H}_0$ is the output of the hidden layer and $\mathbf{P}_0 = \left(\mathbf{H}_0^T\mathbf{H}_0\right)^{-1}$.

In the online learning phase, when the first set of training data arrives, the hidden layer output can be obtained, so the output layer weights can be expressed as

$$\begin{aligned}\mathbf{P}_{k+1} &= \mathbf{P}_k - \mathbf{P}_k\mathbf{H}_{k+1}^T\left(\mathbf{I} + \mathbf{H}_{k+1}\mathbf{P}_k\mathbf{H}_{k+1}^T\right)^{-1}\mathbf{H}_{k+1}\mathbf{P}_k \\ \beta^{(k+1)} &= \beta^{(k)} + \mathbf{P}_{k+1}\mathbf{H}_{k+1}^T\left(\mathbf{Y}_{k+1} - \mathbf{H}_{k+1}\beta^{(k)}\right).\end{aligned} \tag{6}$$

In this case, the number of training data arriving in each group can be inconsistent.

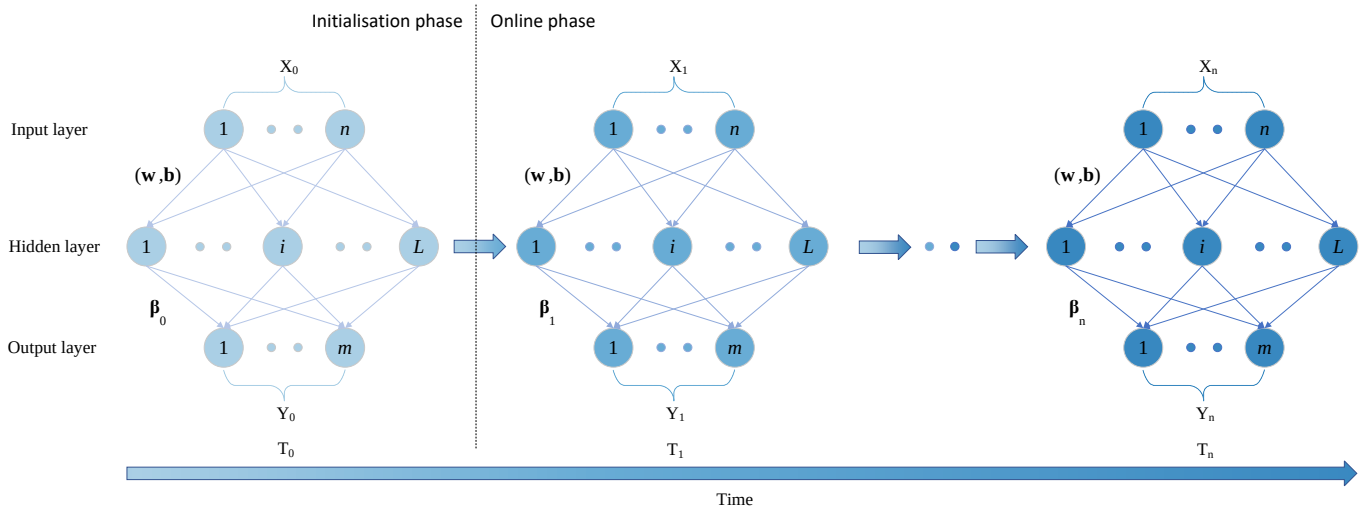

Figure 3. Main architecture of OS-ELM.

4. The Proposed Method

In this section, we first explore the fingerprint similarity problem and the effect of environmental changes to the signal in DFL to formulate the problem description. The overview and details of the proposed method are then demonstrated, respectively.

4.1. Problem Description

In the time-varying environment, the accuracy of fingerprint-based DFL mainly depends on the quality of the fingerprint and the adaptability of the model. The distinguishability of fingerprints corresponding to different locations directly affects the accuracy of DFL. Since the bandwidth of WiFi cards is limited, for example, the Intel 5300 NIC has a bandwidth of up to 40 MHz, it directly limits the sensing ability of the WiFi signal, which leads to fingerprint similarity problem. At the same time, the multipath effect of the

indoor environment worsens this problem. We use the resonance strength to quantify the distinguishability between reference points (see Figure 4) [15].

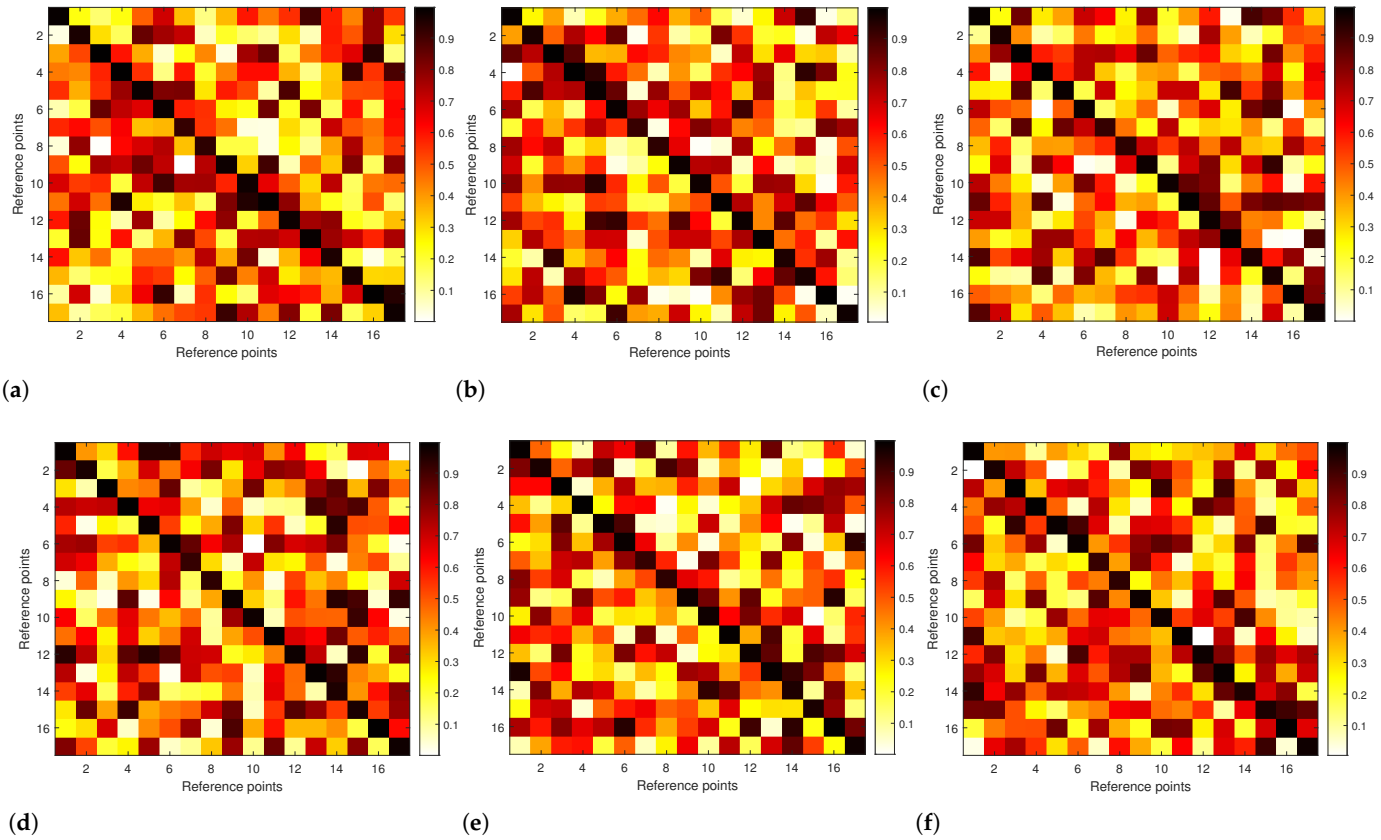

Figure 4. Resonance strength between reference points of different antenna pairs: (**a**) Signal between the first transmitting antenna and the first receiving antenna; (**b**) Signal between the first transmitting antenna and the second receiving antenna; (**c**) Signal between the first transmitting antenna and the third receiving antenna; (**d**) Signal between the second transmitting antenna and the first receiving antenna; (**e**) Signal between the second transmitting antenna and the second receiving antenna; (**f**) Signal between the second transmitting antenna and the third receiving antenna.

In Figure 4a, both the X-axis and Y-axis indicate reference points, and we use the CSI of 30 subcarriers between the first transmitting antenna and the first receiving antenna to calculate the resonance strength between different reference points. The signal with high similarity has a larger strength, up to 1. In this paper, we use two transmitting antennas and three receiving antennas, so there are six combinations, as shown in Figure 4a–f. From Figure 4, we can find that even with different antenna pairs, there is a certain degree of similarity between different reference points. Therefore, designing discriminable fingerprints is an important challenge.

Additionally, during long-term indoor localization, the interaction between the target and the environment will have an impact on the environment and cause the environment to change. The environmental changes will affect the propagation of WiFi signals, causing the changes of fingerprints and affecting the accuracy of DFL. In the time-varying indoor environment, the WiFi signal is mainly affected by the following three factors:

(a) Due to the asynchronous clocks between transceivers, there exist random initial phase offsets caused by WiFi NIC initialization when the transceiver device is restarted.
(b) The change of signal distribution when the transceiver is moved unintentionally.
(c) Indoor multipath effect changes when the location of items in the indoor environment changes, which affects the signal propagation path.

We used data from one of the thirty subcarriers in the CSI over a period of time to compare the raw signal with the changed signal when the environment has changed, as shown in Figure 5, where the X-axis and Y-axis indicate the real and imaginary parts of the CSI signal, respectively. From Figure 5a, we can find that the signal has shifted when the device is powered off and restarted. But when the transceiver is moved by chance, the signal changes dramatically and will affect the fingerprints, which is shown in Figure 5b. Any change in the indoor environment will cause changes of the signal, which will affect the localization performance. Therefore, it is necessary to design an adaptive model and update it regularly. The adaptability of the model directly determines its ability to adapt to changes in the time-varying indoor environment.

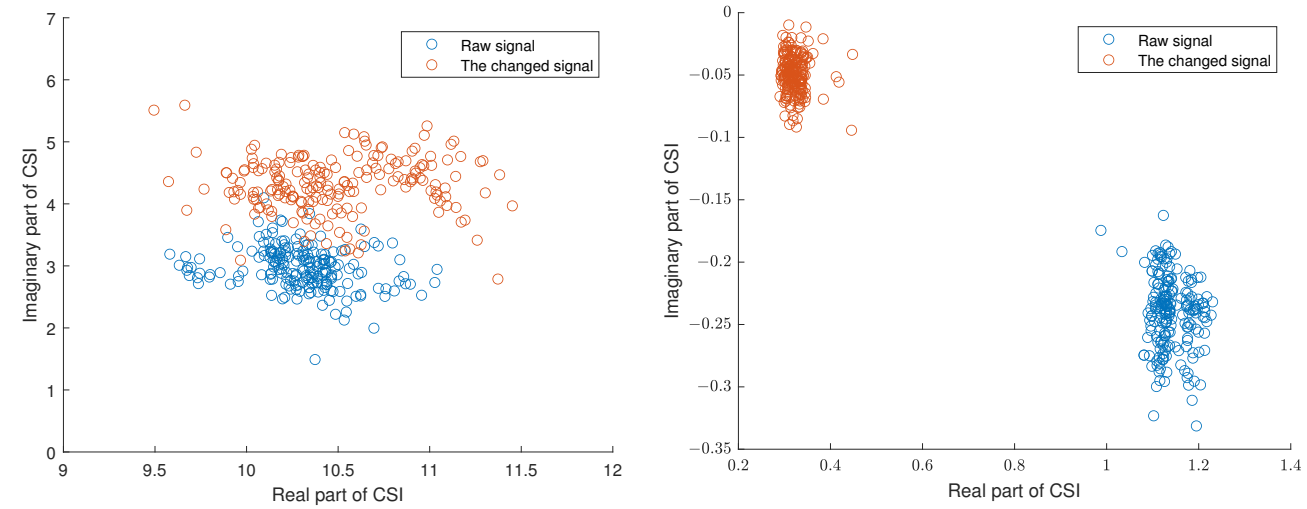

(**a**) (**b**)

Figure 5. Signal changes caused by environmental changes: (**a**) Signal changes when the transceiver device is restarted; (**b**) Signal changes when the transceiver is moved.

4.2. The Overview of DFL Based on ML-OSELM

In the time-varying environment, the propagation pattern of WiFi signals will change. In order to adapt to such changes and ensure the accuracy of DFL in the time-varying environments, we propose a DFL method based on ML-OSELM, which is shown in Figure 6.

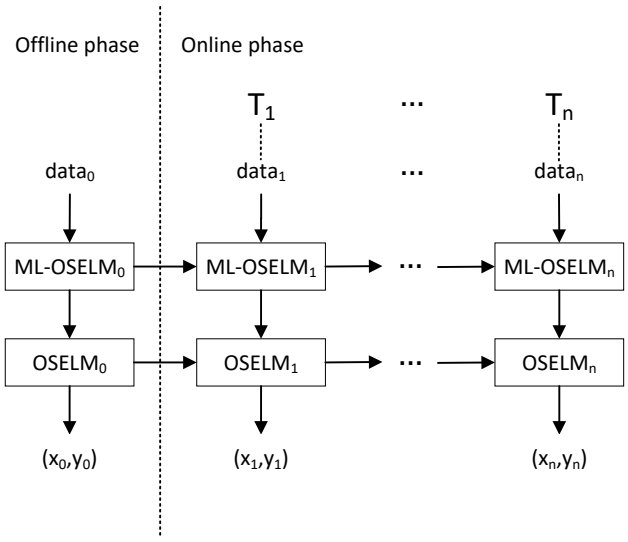

Figure 6. The overview of ML-OSELM-based DFL.

The proposed method consists of two phases, which are the offline phase and the online phase. In the offline phase, WiFi CSI signals are first collected, and the collected data are then transformed into weight-based fingerprints by ML-OSELM. We replace the original CSI with the hidden layer parameters of ML-OSELM as fingerprints. The CSI of each reference point is trained using ML-OSELM separately to obtain the corresponding weight-based fingerprints, which are constructed as a weight-based fingerprint database. Finally, the new fingerprints are used as input and trained using OS-ELM to obtain the adaptive DFL model.

The online phase is divided into two cases: online localization phase and online learning phase. In the online localization phase, when real-time data are collected, it is first transformed into weight-based fingerprints using ML-OSELM and then fed into the model trained in the offline phase to obtain the location of the target. When the environment changes, we collect data from the new environment and use it to update the model to adapt to the environment, and we call this phase the online learning phase. During the online learning phase, the weights and biases of the model are fine-tuned to adapt to the changed environment.

4.3. Deep Representations for the Fingerprints

ML-OSELM is stacked by Online Sequential Extreme Learning Machine-Autoencoder (OS-ELM-AE) [32]. In OS-ELM-AE, the parameters of the input layer and the hidden layer bias are randomly generated and orthogonal. OS-ELM-AE is an unsupervised learning algorithm, and its inputs are also its outputs [33]. Therefore, the output weights of its initialization phase can be expressed as

$$\beta^{(0)} = \mathbf{P}_0 {\mathbf{H}_0}^T \mathbf{X}_0. \tag{7}$$

In the online learning phase, when the $(k+1)$th set of training data arrives, the weights $\beta^{(k+1)}$ can be expressed as

$$\begin{aligned} \mathbf{P}_{k+1} &= \mathbf{P}_k - \mathbf{P}_k \mathbf{H}_{k+1}^T \left(\mathbf{I} + \mathbf{H}_{k+1} \mathbf{P}_k \mathbf{H}_{k+1}^T \right)^{-1} \mathbf{H}_{k+1} \mathbf{P}_k \\ \beta^{(k+1)} &= \beta^{(k)} + \mathbf{P}_{k+1} \mathbf{H}_{k+1}^T \left(\mathbf{X}_{k+1} - \mathbf{H}_{k+1} \beta^{(k)} \right). \end{aligned} \tag{8}$$

In ML-OSELM, the parameters of all hidden layers can be initialized by Equation (7), and Equation (8) can be used to train online for subsequent arrivals of data. The output of the hidden layer l for the $(k+1)$th set of data can be expressed as

$$\mathbf{H}_k^l = g\left(\left(\beta_l^{(k)} \right)^T \mathbf{H}_k^{l-1} \right), \tag{9}$$

where $g(\cdot)$ denotes the activation function, and $\beta_l^{(k)}$ denotes the output weights of OS-ELM-AE in the hidden layer l of the kth data set. The input layer can be considered as the zeroth hidden layer. ML-OSELM is divided into two phases as follows.

(1) Initialization phase

In this phase, for ML-OSELM with p hidden layers, the output of hidden layer l is computed as

$$\mathbf{H}_0^l = g\left(\left(\beta_l^{(0)} \right)^T \mathbf{H}_0^{l-1} \right), l = 1, 2, \ldots, p, \tag{10}$$

where $\beta_l^{(0)}$ can be obtained by Equation (7). The parameters of the hidden layer p to the output layer is calculated as

$$\beta_p^0 = \mathbf{P}_0 (\mathbf{H}_0^p)^T \mathbf{Y}_0. \tag{11}$$

(2) Online learning phase

In this phase, when the $(k+1)$th set of training data arrives, the output of the hidden layer l is obtained by

$$\mathbf{H}_{k+1}^{l} = g\left(\left(\beta_{l}^{(k+1)}\right)^{T}\mathbf{H}_{k+1}^{l-1}\right), l = 1, 2, \ldots, p, \tag{12}$$

where $\beta_{l}^{(k+1)}$ can be obtained by Equation (8). The weights of the output layer are calculated as

$$\beta^{(k+1)} = \beta^{(k)} + \mathbf{P}_{k+1}\mathbf{H}_{k+1}^{T}\left(\mathbf{Y}_{k+1} - \mathbf{H}_{k+1}\beta^{(k)}\right), \tag{13}$$

where $\mathbf{H}_{k+1} = \mathbf{H}_{k+1}^{p}$ can be obtained by Equation (12).

As mentioned above, to alleviate the fingerprint similarity problem, we use ML-OSELM to transform the original signal into a discriminable fingerprint. Specifically, we use the weights of ML-OSELM as the new fingerprint (see Algorithm 1). This method can help tackle the similarity problem because we use CSI as input during the training process, and this method can learn data with multilayer autoencoders. Therefore, the weights of ML-OSELM contain information about the target position, and we use the weights to replace the raw signal as the new fingerprint. This deep representation method can help improve the localization performance.

Algorithm 1 Weight-Based Fingerprint Representations

Input: N packet receptions for each of the q training locations of the $(k+1)$th set of data;
Output: q groups of fingerprints corresponding to q locations of the $(k+1)$th set of data;

Initialization:
for $i = 1; i <= q$ **do**
  //Make the input data X^0 as the 0th hidden layer;
  Set $H^0 = X^0$;
  Randomly initialize w, b, where $w^{\mathrm{T}}w = 1$ and $\mathrm{b}^{\mathrm{T}}\mathrm{b} = 1$;
  //p is the number of hidden layers;
  for $l = 1; l <= p$ **do**
    $H_0 = g(wH_0^{l-1} + b)$;
    $P_0 = \left(H_0^T H_0\right)^{-1}$;
    $\beta_l^0 = P_0(H_0)^T(H_0^{l-1})$;
    $H_0^l = g\left(\left(\beta_l^0\right)^T H_0^{l-1}\right), l = 1, 2, \ldots, p$;
  end for
  //Obtain $Fingerprint_i$;
  $Fingerprint_i \leftarrow [\beta_1^0, \ldots, \beta_p^0]$;
end for
Sequential Learning:
//K is the number of data sets;
for $k = 0; k <= K$ **do**
  for $i = 1; i <= q$ **do**
    //Make the input data X^0 as the 0th hidden layer;
    Set $H^k = X^k$;
    //p is the number of hidden layers;
    for $l = 1; l <= p$ **do**
      $H_k = g(wH_k^{l-1} + b)$;
      $P_k = \left(H_k^T H_k\right)^{-1}$;
      $\beta_l^k = P_k(H_k)^T(H_k^{l-1})$;
      $H_k^l = g\left(\left(\beta_l^k\right)^T H_k^{l-1}\right), l = 1, 2, \ldots, p$;
    end for
    //Obtain $Fingerprint_i$;
    $Fingerprint_i \leftarrow [\beta_1^k, \ldots, \beta_p^k]$;
  end for
end for

5. Performance Verification

5.1. Experimental Setup

In this paper, we build a device-free localization system using Intel 5300 NIC in the time-varying indoor environment. We use a miniPC with Intel 5300 NIC as the receiver and a commercial router (i.e., TP-Link WDR5300) as the transmitter. The transmitter is equipped with two antennas, while the receiver has three antennas, so each data packet contains $3 \times 2 \times 30$: a total of 180 CSI values. In order to collect the raw CSI, we use CSITOOL [34] under the Linux system to collect the signal of the target at different reference points. We divide the cells in the monitoring area and select the reference location uniformly. The reference points are set to the center of each cell as the blue dots and the testing points are the centers of the reference point as the red squares, where the cell size is 1 m by 1 m. The layout of the floor plan of the experimental environment is shown as Figure 7, where the transceiver is located at the place with the mark "TX" and the receiver is located at the place with the mark "RX". Since the fingerprint is highly dependent on the target being trained, we have consistently used the same volunteer as the target for the experiments. During the offline phase, we build a fingerprint database by collecting CSI data when the target is located at the reference points, which is indicated by the blue points. During the online phase, we build the testing set by collecting CSI data when the target is located at the testing points, which is indicated by the red points in Figure 7. In the paper, the experiments are post-processing after the data have been collected.

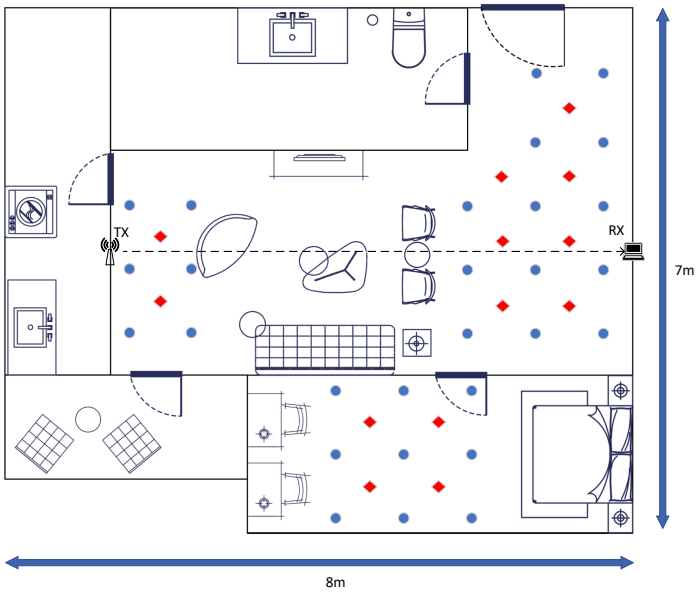

Figure 7. Layout of the experimental scenario. The blue points are reference points and the red points are testing points.

5.2. Performance Evaluation of ML-OSELM-Based DFL Model

Since the collected CSI contains information such as system noise and environmental noise, we must eliminate the noise to enhance CSI quality. Firstly, outliers are abnormal in the signal, so we use the Hampel filter [35] to filter out the outliers. Secondly, noise is generally of high frequency, and hence, it is removed using a moving average filter. The CSI signal may be lost during WiFi signal transmission due to the multipath effect, the NLOS effect, and complex environments. Therefore, we use a one-dimensional linear interpolation algorithm to complement the missing values.

We first verify the effectiveness of weight-based fingerprints. We collect data for a total of five days to design the experiment and compare the weight-based fingerprints with the raw signals and ratio-based fingerprints. The localization performance is shown in Figure 8, where the Y-axis indicates the localization accuracy. We can find that the proposed

weight-based fingerprints can significantly improve the localization performance at all time points.

The localization accuracy is evaluated using the root mean square error (RMSE) defined as

$$RMSE = \sqrt{\frac{1}{N}\sum_{i=1}^{N}(\hat{l}_i - l_i)^2}, \tag{14}$$

where l_i denotes the true location of the ith fingerprint and $\hat{l}_i$ denotes the estimated location of the ith fingerprint. We update the DFL model once at an interval of 4 h, respectively. The effects of DFL by different methods are shown in Figure 9a, where the X-axis indicates the moment of updating the DFL model and the Y-axis indicates the localization accuracy. It can be found that the proposed method outperforms the other methods. The optimal parameters of different methods are shown in Table 1, and we utilize these parameters for localization every 4 h in a day. The cumulative distribution function (CDF) of the localization error in an indoor environment at different moments is given in Figure 9b–f, respectively. From Figure 9b–f, it can be found that the localization performance of the proposed method in this paper is generally better than other methods. Specifically, the proposed method can still achieve an average localization error of about 1.0 m in the indoor environment with rich multipath and shadowing effects, but the average localization error of SVM, random forest, decision tree and BPNN is worse. With the time passing, the environment may change and the accuracy of other methods decreases, while the proposed method still maintains high localization performance due to its strong adaptability. Meanwhile, in Table 2, we show the comparison between the actual positions of some reference points and the estimated positions of other methods, from which we can find that the proposed method has higher accuracy. Obviously, the device-free localization method based on ML-OSELM achieves higher adaptability in a time-varying environment and better localization performance.

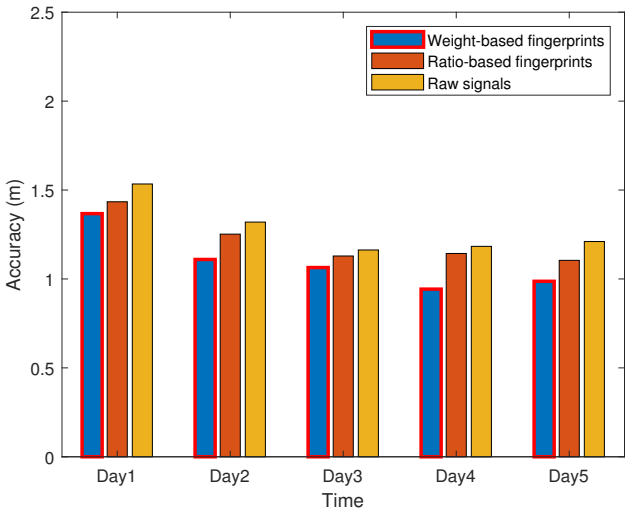

Figure 8. Performance comparison between raw signals, ratio-based fingerprints and weight-based fingerprints.

Table 1. The optimal parameters of different methods.

Methods	Hyperparameters
The proposed method	Activation Function: sigmod; Hidden Layer Nodes: 85
SVM	Kernel: Gaussian; Box Constraint: 466.01; Kernel Scale: 29.72
Random Forest	NumTrees: 160; MinLeafSize: 5
Decision Tree	MinParent: 10; MinLeaf: 4
BPNN	Activation Function: sigmod; Hidden Layer Nodes: 100

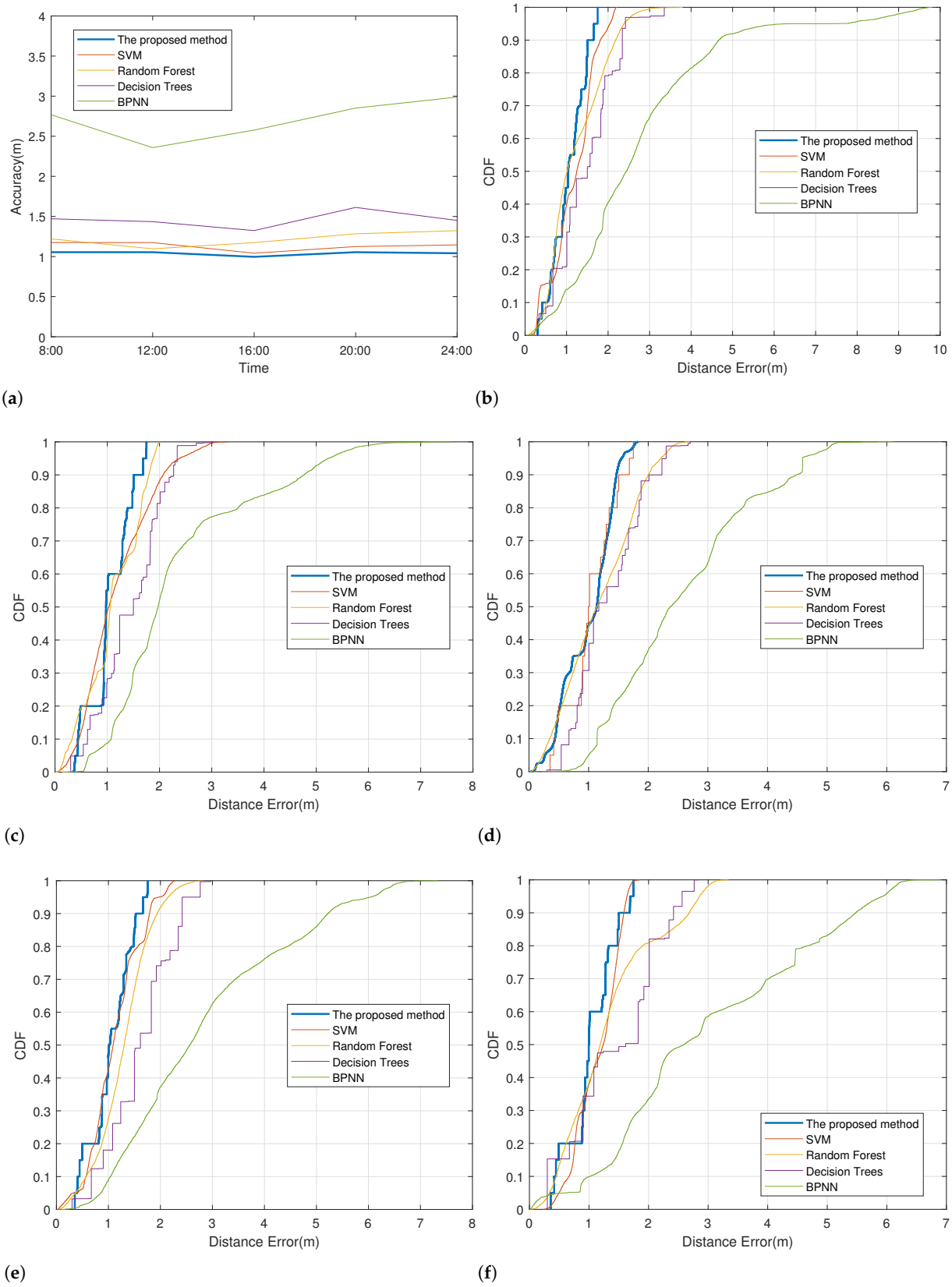

Figure 9. Performance of DFL at different moments: ((**a**) Comparison of the accuracy of each method at different times of day; (**b**–**f**) CDF curves for different methods at each moment of a 4 h interval from 8 to 24 o'clock).

Table 2. The comparison of localization accuracy with different methods.

Location Number	Actual Position	Estimated Position by Existing Approach	Estimated Position by Proposed Approach	RMSE with Existing Approach (in Meter)	RMSE with Proposed Approach (in Meter)
1	(2.4, 2.1)	(2.1, 1.2)	(2.2, 1.9)	0.96	0.35
2	(1.8, 3.6)	(1.2, 2.6)	(1.0, 4.0)	1.10	0.89
3	(2.4, 2.7)	(3.4, 1.4)	(2.7, 3.5)	1.69	0.88
4	(1.2, 0.9)	(3.3, 1.6)	(2.6, 1.8)	2.29	1.75

6. Conclusions

In the time-varying indoor environment, the complex multipath effect will lead to a fingerprint similarity problem, and the environmental changes will cause variations in signal distribution, which may degrade the accuracy of device-free localization (DFL). To address these issues, a device-free localization method is proposed based on the Multilayer Online Sequence Extreme Learning Machine (ML-OSELM). To be specific, a kind of discriminable fingerprint is first designed using the parameters of ML-OSELM. To adapt to environmental changes, an adaptive DFL model is built based on the online sequence extreme learning machine (OS-ELM), which uses weight-based fingerprints as inputs. Experimental results illustrate the high adaptability of the proposed method to the environment, which obtains meter-scale localization accuracy. The proposed approach is used to update the model periodically, being incapable of detecting changes of the environment in a timely manner. In the future work, it is advised that the online DFL model can be studied based on modeling the dynamic changes of the environment to improve the practical applicability of indoor localization.

Author Contributions: Conceptualization, J.X. and Q.C.; Methodology, X.C. and Q.C.; software, J.X. and X.C.; validation, J.X. and Q.C.; formal analysis, Q.C.; investigation, W.X. and Q.C.; resources, W.X. and X.C.; data curation, J.X. and X.C.; writing—original draft preparation, J.X. and X.C.; writing—review and editing, W.X. and Q.C.; supervision, X.C. and W.X. All authors have read and agreed to the published version of the manuscript.

Funding: This work was supported in part by the National Natural Science Foundations of China (NSFC) under grant 62173032, the Foshan Science and Technology Innovation Special Project under grant BK22BF005, the Regional Joint Fund of the Guangdong Basic and Applied Basic Research Fund under grant 2022A1515140109, and the Natural Science Foundation of Shandong Province under grant ZR202212040125.

Institutional Review Board Statement: Not applicable.

Informed Consent Statement: Not applicable.

Data Availability Statement: The data presented in this study are available on request from the corresponding author. The data are not publicly available due to privacy.

Conflicts of Interest: The authors declare no conflicts of interest.

References

1. Chen, X.; Chen, L.; Feng, C.; Fang, D.; Xiong, J.; Wang, Z. Sensing our world using wireless signals. *IEEE Internet Comput.* **2019**, *23*, 38–45. [CrossRef]
2. Yang, Z.; Zhou, Z.; Liu, Y. From RSSI to CSI: Indoor localization via channel response. *ACM Comput. Surv.* **2013**, *46*, 1–32. [CrossRef]
3. Shit, R.C.; Sharma, S.; Puthal, D.; James, P.; Pradhan, B.; van Moorsel, A.; Zomaya, A.Y.; Ranjan, R. Ubiquitous localization (UbiLoc): A survey and taxonomy on device free localization for smart world. *IEEE Commun. Surv. Tutor.* **2019**, *21*, 3532–3564. [CrossRef]
4. Vasisht, D.; Jain, A.; Hsu, C.Y.; Kabelac, Z.; Katabi, D. Duet: Estimating user position and identity in smart homes using intermittent and incomplete RF-data. *Proc. ACM Interact. Mobile Wearable Ubiquitous Technol.* **2018**, *2*, 1–21. [CrossRef]
5. LinkSys Aware. Available online: https://www.linksys.com/noname/software-and-services/linksys-aware/ (accessed on 7 January 2023).

6. Qian, K.; Wu, C.; Zhang, Y.; Zhang, G.; Yang, Z.; Liu, Y. Widar2.0: Passive human tracking with a single Wi-Fi link. In Proceedings of the International Conference on Mobile Systems, Applications, and Services, Munich, Germany, 10–15 June 2018; pp. 350–361.
7. Lashkari, B.; Rezazadeh, J.; Farahbakhsh, R.; Sandrasegaran, K. Crowdsourcing and sensing for indoor localization in IoT: A review. *IEEE Sens. J.* **2018**, *19*, 2408–2434. [CrossRef]
8. Renaudin, V.; Ortiz, M.; Perul, J.; Torres-Sospedra, J.; Jiménez, A.R.; Pérez-Navarro, A.; Mendoza-Silva, G.M.; Seco, F.; Landau, Y.; Marbel, R.; et al. Evaluating indoor positioning systems in a shopping mall: The lessons learned from the IPIN 2018 competition. *IEEE Access* **2019**, *7*, 148594–148628. [CrossRef]
9. Jondhale, S.R.; Jondhale, A.S.; Deshpande, P.S.; Lloret, J. Improved trilateration for indoor localization: Neural network and centroid-based approach. *Int. J. Distrib. Sens. Netw.* **2021**, *17*, 15501477211053997. [CrossRef]
10. Wang, J.; Zhang, X.; Gao, Q.; Yue, H.; Wang, H. Device-free wireless localization and activity recognition: A deep learning approach. *IEEE Trans. Veh. Technol.* **2016**, *66*, 6258–6267. [CrossRef]
11. Nkabiti, K.P.; Chen, Y. Application of solely self-attention mechanism in CSI-fingerprinting-based indoor localization. *Neural Comput. Appl.* **2021**, *33*, 9185–9198. [CrossRef]
12. Wang, Z.; Guo, B.; Yu, Z.; Zhou, X. Wi-Fi CSI-based behavior recognition: From signals and actions to activities. *IEEE Commun. Mag.* **2018**, *56*, 109–115. [CrossRef]
13. Ding, J.; Wang, Y.; Si, H.; Gao, S.; Xing, J. Three-Dimensional Indoor Localization and Tracking for Mobile Target Based on WiFi Sensing. *IEEE Internet Things J.* **2022**, *9*, 21687–21701. [CrossRef]
14. Khalilsarai, M.B.; Stefanatos, S.; Wunder, G.; Caire, G. WiFi-Based Indoor Localization via Multi-Band Splicing and Phase Retrieval. In Proceedings of the IEEE International Workshop on Signal Processing Advances in Wireless Communications (SPAWC), Cannes, France, 2–5 July 2019; pp. 1–5. [CrossRef]
15. Wu, Z.H.; Han, Y.; Chen, Y.; Liu, K.R. A time-reversal paradigm for indoor positioning system. *IEEE Trans. Veh. Technol.* **2015**, *64*, 1331–1339. [CrossRef]
16. Xue, J.; Zhang, J.; Gao, Z.; Xiao, W. Enhanced WiFi CSI Fingerprints for Device-Free Localization With Deep Learning Representations. *IEEE Sens. J.* **2022**, *23*, 2750–2759. [CrossRef]
17. Zhang, G.; Zhang, D.; He, Y.; Chen, J.; Zhou, F.; Chen, Y. Multi-Person Passive WiFi Indoor Localization with Intelligent Reflecting Surface. *IEEE Trans. Wirel. Commun.* **2023**, *22*, 6534–6546. [CrossRef]
18. Kandel, L.N.; Yu, S. VWAN: Virtual WiFi ANtennas for Increased Indoor Localization Accuracy. In Proceedings of the IEEE International Conference on Industrial Internet (ICII), Orlando, FL, USA, 11–12 November 2019; pp. 258–267. [CrossRef]
19. Zuo, X.; Tian, Z.; Zhou, M.; Jin, Y.; Li, Z. Two-Stage Multi-Dimensional Parameters Estimation for Device-Free Human Tracking using WiFi Signals. In Proceedings of the International Symposium on Antennas and Propagation and USNC-URSI Radio Science Meeting, Denver, CO, USA, 10–15 July 2022; pp. 748–749. [CrossRef]
20. Zhang, L.; Wang, H. Device-Free Tracking via Joint Velocity and AOA Estimation With Commodity WiFi. *IEEE Sens. J.* **2019**, *19*, 10662–10673. [CrossRef]
21. Ding, J.; Wang, Y.; Fu, S.; Si, H.; Zhang, J.; Gao, S. Multiview Features Fusion and AdaBoost Based Indoor Localization on WiFi Platform. *IEEE Sens. J.* **2022**, *22*, 16607–16616. [CrossRef]
22. Zhang, J.; Xiao, W.; Li, Y. Data and knowledge twin driven integration for large-scale device-free localization. *IEEE Internet Things J.* **2020**, *8*, 320–331. [CrossRef]
23. Wei, W.; Yan, J.; Wu, X.; Wang, C.; Zhang, G. A Data Preprocessing Method for Deep Learning-Based Device-Free Localization. *IEEE Commun. Lett.* **2021**, *25*, 3868–3872. [CrossRef]
24. Shi, S.; Sigg, S.; Chen, L.; Ji, Y. Accurate Location Tracking From CSI-Based Passive Device-Free Probabilistic Fingerprinting. *IEEE Trans. Veh. Technol.* **2018**, *67*, 5217–5230. [CrossRef]
25. Duan, Y.; Lam, K.Y.; Lee, V.C.S.; Nie, W.; Liu, K.; Li, H.; Xue, C.J. Data Rate Fingerprinting: A WLAN-Based Indoor Positioning Technique for Passive Localization. *IEEE Sens. J.* **2019**, *19*, 6517–6529. [CrossRef]
26. Zeng, Y.; Wu, D.; Xiong, J.; Yi, E.; Gao, R.; Zhang, D. FarSense: Pushing the Range Limit of WiFi-Based Respiration Sensing with CSI Ratio of Two Antennas. *Proc. ACM Interact. Mobile Wearable Ubiquitous Technol.* **2019**, *3*, 1–26. [CrossRef]
27. Zhou, R.; Hou, H.; Gong, Z.; Chen, Z.; Tang, K.; Zhou, B. Adaptive Device-Free Localization in Dynamic Environments Through Adaptive Neural Networks. *IEEE Sens. J.* **2021**, *21*, 548–559. [CrossRef]
28. Lei, Q.; Zhang, H.; Sun, H.; Tang, L. Fingerprint-Based Device-Free Localization in Changing Environments Using Enhanced Channel Selection and Logistic Regression. *IEEE Access* **2018**, *6*, 2569–2577. [CrossRef]
29. Zhang, J.; Li, Y.; Xiong, H.; Dou, D.; Miao, C.; Zhang, D. HandGest: Hierarchical Sensing for Robust in-the-air Handwriting Recognition with Commodity WiFi Devices. *IEEE Internet Things J.* **2022**, *9*, 19529–19544. [CrossRef]
30. Yan, J.; Wan, L.; Wei, W.; Wu, X.; Zhu, W.P.; Lun, D.P.K. Device-Free Activity Detection and Wireless Localization Based on CNN Using Channel State Information Measurement. *IEEE Sens. J.* **2021**, *21*, 24482–24494. [CrossRef]
31. Liang, N.Y.; Huang, G.B.; Saratchandran, P.; Sundararajan, N. A fast and accurate online sequential learning algorithm for feedforward networks. *IEEE Trans. Neural Netw.* **2006**, *17*, 1411–1423. [CrossRef]
32. Mirza, B.; Kok, S.; Dong, F. Multi-layer online sequential extreme learning machine for image classification. In Proceedings of the Extreme Learning Machine, Hangzhou, China, 15–17 December 2015; pp. 39–49.
33. Zhang, J.; Li, Y.; Xiao, W.; Zhang, Z. Non-iterative and fast deep learning: Multilayer extreme learning machines. *J. Franklin Inst.* **2020**, *357*, 8925–8955. [CrossRef]

34. Halperin, D.; Hu, W.; Sheth, A.; Wetherall, D. Tool release: Gathering 802.11 n traces with channel state information. *ACM SIGCOMM Comp. Commun. Rev.* **2011**, *41*, 53. [CrossRef]
35. Davies, L.; Gather, U. The identification of multiple outliers. *J. Am. Stat. Assoc.* **1993**, *88*, 782–792. [CrossRef]